

1 **Title:** Effects of medical resource capacities and intensities of public
2 mitigation measures on outcomes of COVID-19 outbreaks

3 **One sentence summary:** Multiple data sources and cross validation of a COVID-19
4 epidemic model, coupled with a medical resource logistic model, reveal that the key
5 factors that affect epidemic progressions and their outbreak patterns in different
6 countries are the type of emergency medical response to avoid runs on medical
7 resources, especially improved detection rates, the ability to promote public health
8 measures, and the synergistic effects of combinations of multiple prevention and
9 control strategies.

10

11 **Authors:** Xia Wang^{1#}, Qian Li^{2#}, Xiaodan Sun^{2#}, Sha He¹, Fan Xia², Pengfei
12 Song², Yiming Shao³, Jianhong Wu⁴, Robert A. Cheke^{5*}, Sanyi Tang^{1*}, Yanni
13 Xiao^{2*}

14

15 **Affiliations:**

16 ¹School of Mathematics and Information Sciences, Shaanxi Normal University, Xi'an,
17 710119, P.R. China. ²Department of Applied Mathematics, Xi'an Jiaotong University,
18 Xi'an 710049, P.R. China. ³Chinese Center for Disease Control and Prevention,
19 Beijing 102206, P.R. China. ⁴Laboratory for Industrial and Applied Mathematics,
20 Department of Mathematics and Statistics, York University, Toronto, Ontario, M3J
21 1P3, Canada. ⁵Natural Resources Institute, University of Greenwich at Medway,
22 Central Avenue, Chatham Maritime, Kent, ME4 4TB, UK.

23 #These authors contributed equally to this work

24 *Corresponding author. Email: r.a.cheke@greenwich.ac.uk;

25 NOTE: This preprint reports new research that has not been certified by peer review and should not be used to guide clinical practice.

26 **Abstract:**

27 The COVID-19 pandemic is complex and is developing in different ways according to
28 the country involved. To identify the key parameters or processes that have the greatest
29 effects on the pandemic and reveal the different progressions of epidemics in different
30 countries, we quantified enhanced control measures and the dynamics of the production
31 and provision of medical resources. We then nested these within a COVID-19 epidemic
32 transmission model, which is parameterized by multi-source data. We obtained rate
33 functions related to the intensity of mitigation measures, the effective reproduction
34 numbers and the timings and durations of runs on medical resources, given differing
35 control measures implemented in various countries. Increased detection rates may
36 induce runs on medical resources and prolong their durations, depending on resource
37 availability. Nevertheless, improving the detection rate can effectively and rapidly
38 reduce the mortality rate, even after runs on medical resources. Combinations of
39 multiple prevention and control strategies and timely improvement of abilities to
40 supplement medical resources are key to effective control of the COVID-19 epidemic.
41 A 50% reduction in comprehensive control measures would have led to the cumulative
42 numbers of confirmed cases and deaths exceeding 590000 and 60000, respectively, by
43 27 March 2020 in mainland China. The proposed model can assist health authorities to
44 predict when they will be most in need of hospital beds and equipment such as
45 ventilators, personal protection equipment, drugs and staff.

46

47

48

49

50

51

52

53

54

55

56

57 **Main Text:**

58 In the absence of effective treatments for, or vaccines against, COVID-19, the early
59 adoption of strict prevention and control measures will undoubtedly play a very
60 important role in limiting the spread of the virus and the growth of the epidemic (1-8).
61 This has been shown by the successes of China, South Korea and other countries in
62 curbing the spread of the virus and achieving important prevention and control results
63 (7, 8). For example, unprecedented restrictive measures, including travel restrictions,
64 contact tracing, quarantine and lock-down of entire towns/cities adopted by the Chinese
65 authorities has resulted in a significant reduction in the COVID-19 epidemic in
66 mainland China (7, 8). However, with the increase of COVID-19 cases in the world,
67 especially the sharp increase in the cumulative number of reported deaths, the shortage
68 of medical resources has become the most serious threat facing countries experiencing
69 serious epidemics.

70 Enhancing the detection rate can lead to early quarantine or isolation of latent and/or
71 infected individuals and then the numbers of confirmed cases (2, 5, 8) increase
72 significantly. A common problem faced by many countries is to what extent can
73 improvements to medical resources be synchronized with an increase of patient
74 numbers, in order to avoid runs on medical resources. How to quantify the levels of
75 improvements in prevention and control measures and of medical resources in order to
76 reveal differences in the epidemic's progression in different countries remain unclear,
77 but are addressed in this study. In order to investigate this issue, we propose a general
78 COVID-19 epidemic transmission dynamics model that includes limitations of medical
79 resources and enhancing prevention and control strategies in six selected countries
80 (China, South Korea, Japan, Italy, Spain and Iran) (7, 8). The formulated transmission
81 model is parameterized by multi-source data such as the numbers of newly reported
82 cases and the cumulative numbers of deaths for each country.

83 Using information such as the number of beds per thousand people in each country
84 and differences in increasing volumes of medical resources (closely related to medical
85 staff numbers) that can be provided by each country during public health emergencies
86 (9-14), we modeled the number of beds provided by each country during the
87 development of a COVID-19 epidemic with the logistic growth function using country-
88 specific varying growth rates and carrying capacities (section SM1 of Supplementary
89 material (SM)). In order to represent the limitation of hospital beds we divided
90 confirmed cases into two groups in terms of severity of symptoms: non-hospitalized

91 and hospitalized. The non-hospitalized individuals, who may later be admitted to
92 hospital depending on the number of hospital beds available, can become a new source
93 of infection, leading to new cases including family cluster infections. Hence the
94 dynamics of hospital beds need to be nested within the transmission dynamic model to
95 examine the level of improvement in medical resources on a COVID-19 epidemic in
96 each country studied.

97 The multiple data sources including the numbers of newly reported cases and the
98 cumulative numbers of reported deaths for all six countries were used to estimate the
99 unknown parameters and to fit the data (Figs.1 and S2, Table S2). The parameter values
100 associated with the intensity of disease transmission in each country are compared and
101 discussed in SM3. Like China, the epidemic in South Korea is almost stable, and their
102 respective effective reproduction numbers have, by mid-April 2020, both been less than
103 1 for six weeks (Fig.1 (B, C)). The COVID-19 epidemic in Japan has been fluctuating
104 on a small scale with a lot of random fluctuations. However, since 25 March, the
105 epidemic has rebounded, the numbers of newly reported cases and deaths have
106 continued to increase (Figs.1(D) and S2(C)). The Italian and Spanish epidemics seem
107 to be about to peak and they are approaching their turning points, but their cumulative
108 death rates will continue to rise, and there is no sign of stabilization in the short term
109 (Figs.1(E, F) and S2(D, E)). Finally, the epidemic in Iran has a strange trend, with
110 repeated and huge fluctuations (Figs.1(G) and S2(F)).

111 In order to reveal the complex patterns and huge differences in the COVID-19
112 epidemics among the various countries shown in Figs.1 and S2, we compared the
113 effectiveness and timeliness of the continuously strengthened comprehensive
114 prevention and control strategies in various countries (Fig.2), with a view to increasing
115 our understanding and making suggestions for future prevention and control strategies.
116 To do this, we quantified the intensities of the control measures against COVID-19
117 epidemics for each country by estimating the evolution of contact rate ($c(t)$), quarantine
118 rate ($q(t)$), detection rates ($\delta_I(t)$ and $\delta_T(t)$) and medical resource capacity ($H_c(t)$) (see
119 sections SM2 and SM3).

120 It follows from Fig.2 that five of the six countries, but not Japan, are constantly
121 increasing their numbers of beds available ($H_c(t)$, green curves) for COVID-19 patients
122 with the development of the epidemic in accordance with each country's medical
123 capacity. The rates of increases in the numbers of beds are in the order South Korea,
124 China, Italy, Spain and Iran. South Korea and China would soon be able to reach the
125 maximum number of medical beds needed after their control intensity improvements

126 (Fig.2(A) and (B)). Due to the low rate of increase of infected individuals in Japan, so
127 far there is no urgent need to supplement the number of beds for high-risk patients there
128 (shown in Fig.2(C)). The contact rate function (blue curve in Fig.2) in China has
129 declined very fast since 23 January when Wuhan city and all parts of the country
130 continued to take stringent control measures. The response speed of increasing social
131 distancing and strengthening self-quarantine measures was very fast in mainland China,
132 while South Korea's, Italy's and Spain's contact rate functions gradually decrease. Italy
133 and Spain have relatively low quarantine rates (red curves in Fig.2) while the other four
134 countries all have high contact tracing followed by quarantine. Japan's quarantine rate
135 remains at a high level so far. The relatively high detection rates, followed by strict
136 quarantine, are associated with quick control of the epidemic (as illustrated for China,
137 South Korea and Iran in Fig.2 (A, B, F)) while the epidemics in Italy and Spain with
138 low detection rates became worse (Fig.2 (D, E)).

139 Define $H_r(t) = \max\{H_c(t) - H_2(t) - \theta H_1(t), 0\}$ as the daily potential number of
140 beds available for the individuals currently quarantined at home. Then $H_r(t) = 0$ for
141 certain days means the occurrence of a run on medical resources in some countries. In
142 order to identify the timing of such runs for various countries, reveal the variation in
143 the cumulative number of deaths with the detection rate, maximum number of beds and
144 production capacity of beds, we numerically calculated $H_r(t)$ and the cumulative
145 number of deaths (Fig.3 and Table 1).

146 By calculating $H_r(t)$ with the estimated parameters, we see that the short-term
147 shortage of medical resources in February occurred in mainland China from 1 to 13
148 February. However, after the specially built Huoshenshan Hospital began to treat
149 patients on 4 February and *Fangcang* (shelter/observation ward) hospitals began to treat
150 patients on 5 February, the number of beds increased rapidly, effectively alleviating the
151 shortage of medical resources. However, the cumulative number of deaths would
152 increase by 74.6% (or 137%), if the capacity (or growth rate) of beds were reduced
153 from H_f to $1/3H_f$ (or r_3 to $1/3r_3$) (Fig.3 (A-B) and Table 1). If the two parameters
154 δ_{If} (related to the detection ability) and r_3 were reduced at the same time to $1/3$ of the
155 estimated values, then the duration of the run on medical resources would increase
156 significantly (from 12 days to 37 days) and consequently the cumulative number of
157 deaths would increase rapidly, up to 317.6% by 26 April (Fig.3 (A-B)). If the detection
158 rate is low, the run on resources will occur later, but eventually it will occur in a wider
159 time range, which will lead to more people becoming infected and more deaths. This

160 indicates that rapidly increased supplies of medical resources and disease detection
161 effectively reduced the mortality in China.

162 Increasing the provision of beds ($3r_h$ here) threefold in Italy, Spain and Iran will
163 only alleviate the shortage of resources for a short time, and then the run on medical
164 resources will happen again soon afterwards (green curves in Fig.3 (C,E,G)). Italy and
165 Spain began to recover slowly, after almost 25 days and 15 days, respectively, with zero
166 beds remaining. Iran began to recover at a faster speed after a long period with zero
167 beds remaining. Nevertheless, Iran had the largest reduction in the number of
168 cumulative deaths (a reduction of 20%), followed by Spain (12.8% reduction) (Table
169 1). If the maximum number of beds is only increased to $3H_f$, the results shown in Fig.3
170 clarify that there is little impact on the death toll in Spain and Iran (Fig.3(F, H)).
171 Increases in the detection rate in Italy, Spain and Iran greatly reduces the cumulative
172 number of deaths (red curves in Fig.3(D, F, H)). This is because increasing the detection
173 rate leads to significant declines in the numbers of new infections, due to strict
174 quarantine and isolation strategies, which not only decreases the number of deaths but
175 also avoids runs on medical resources (red curves in Fig.3(C, E)). Furthermore, in Iran
176 increasing the detection rate still induces a run on resources in the early stage of the
177 epidemic but leads to recovery at a later stage due to reduced numbers of new infections
178 (black curves in Fig.3(E)), implicating the weak medical resources in Iran.

179 Having taken continuous and strengthened prevention and control measures, China
180 and South Korea have quickly controlled the epidemic. The key processes for quick
181 mitigation of the epidemic are the intensity of prevention and control measures
182 represented by the four rates r_1 , r_2 , r_3 and r_h : the contact rate declines, quarantine rate
183 increases, decreasing periods for detection and increasing rates of medical resource
184 production, respectively (see SM for explanations). Reducing these rates by 10%, 20%,
185 30%, 40% and 50% simultaneously would have resulted in increased fractions in the
186 cumulative numbers of confirmed cases and deaths (Table 2). Comparing the changing
187 rates indicates that China's control efficacy is better than South Korea's, especially in
188 terms of reducing deaths. Given a reduction by 50% in the comprehensive control
189 measures in China, the cumulative number of confirmed cases and deaths would have
190 exceeded 590000 and 60000, respectively, by 27 March. Therefore, without the very
191 strong and comprehensive prevention and control measures that were invoked (7, 8),
192 the development of China's epidemic would have been unimaginable, with exceedingly
193 large numbers of cases and a surprisingly high death toll.

194 It is known that the marked differences in the epidemics in various countries are
195 associated with differences in the implementation of multiple strategies for public
196 interventions together with increasing medical resource capacities. By estimating time-
197 dependent contact, quarantine and detection rates we quantified enhancements to
198 prevention and control strategies, and modeled the dynamics of medical resources,
199 which were nested within the epidemic model proposed, revealing the timings of runs
200 on medical resources in six different countries. Thus, the model could be used to assist
201 health authorities to predict when they will be most in need of hospital beds, equipment
202 such as ventilators, personal protection equipment (PPE), drugs and medical staff. The
203 model also describes the effect of improving control measures on the complex patterns
204 of epidemics in different countries, shows that detection rates are crucial for reducing
205 morbidity and mortality and that synergies between prevention and control measures
206 and medical resource availability are essential for successful control of COVID-19.

207 Detection of infections is a key process that significantly affects the numbers of
208 confirmed cases and deaths. This is especially so for an increasing detection rate, which,
209 while increasing the number of confirmed cases in the short term, leads to declines in
210 the number of new infections. This is due to strict contact tracing followed by
211 quarantine and isolation, and consequently reductions in the number of confirmed cases
212 and deaths in the long term. Moreover, increasing the detection rate may result in runs
213 on medical resources, depending on their initial capacities. As illustrated in Fig.3 (C, E
214 and G) merely increasing detection rates in Italy or Spain did not induce runs on medical
215 resources but these did occur in Iran (red curves). Hence the synergistic effect of
216 improving medical capacity and production with enhancing detection is essential to
217 mitigating the COVID-19 pandemic as well as avoiding runs on medical resources.

218 We suggest that Japan should pay more attention to increasing medical resources as
219 its detection rate has increased since 25 March, otherwise the numbers of confirmed
220 cases and deaths will increase quickly as the intensity of its control measures is not as
221 high as in South Korea or even in Iran. If Iran had medical conditions equivalent to
222 those of South Korea, the effects of its control measures would be far more effective
223 and the current situation would be less severe. Comparing the estimated rate functions
224 for Italy, Spain and Iran indicates that a low detection rate is a key process that
225 significantly affects the epidemic, while Iran is mainly affected by its limited medical
226 resources. Regardless of other factors, improving the detection rate can effectively and
227 rapidly reduce the mortality rate, even after runs on medical resources. Therefore, in
228 order to effectively reduce the numbers of new infections and mortality in COVID-19

229 outbreaks, detection rates should be increased while improving the production and
230 capacity of medical resources. The synergistic effects of comprehensive prevention and
231 control strategies are likely to succeed in mitigating epidemics, as shown by the
232 experience of China and South Korea (1-3,5-8), from whose examples other countries
233 can learn.

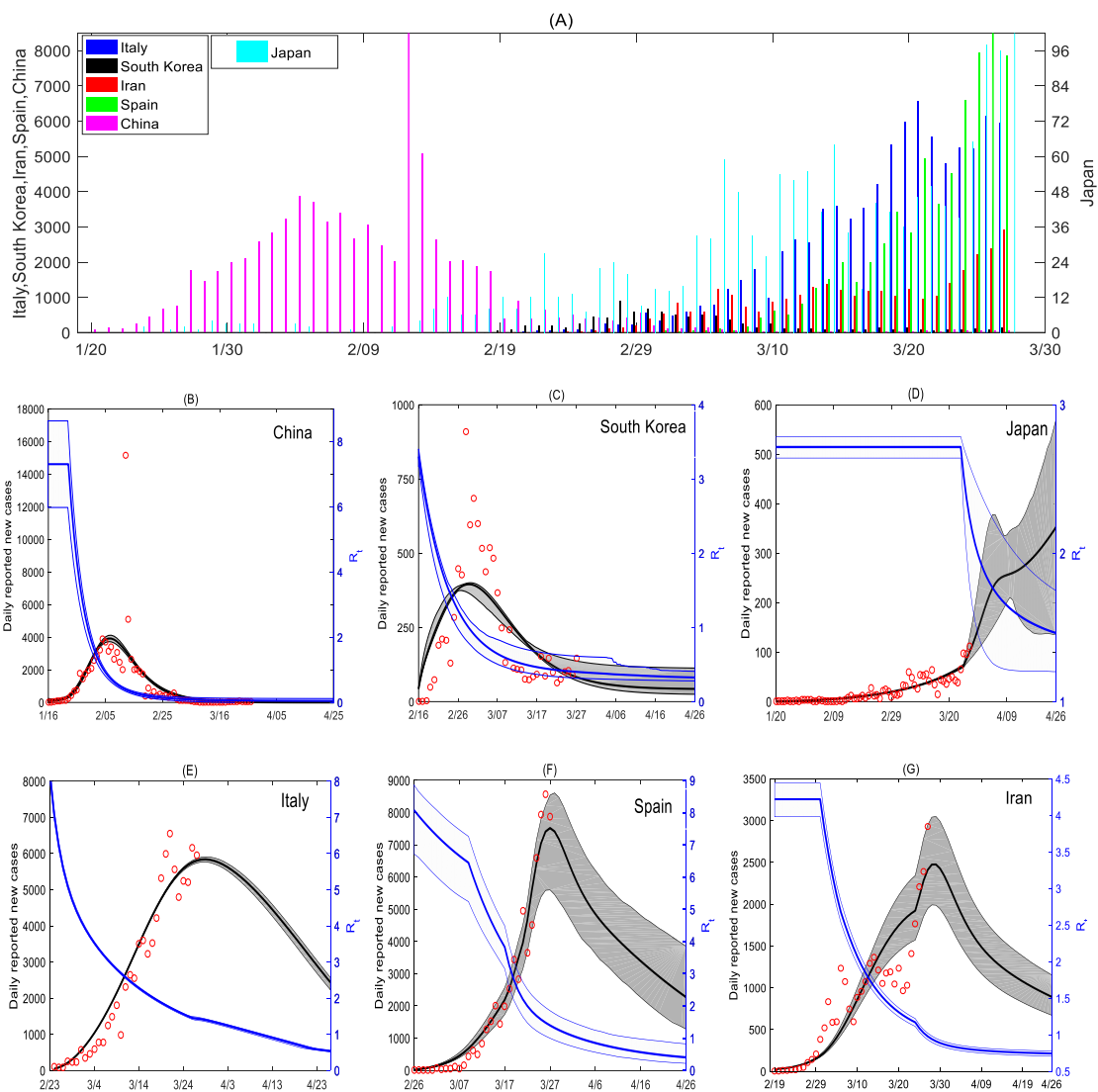
234

235 **References and Notes:**

- 236 1. Chinazzi M. et al. *Science* 2020; 10.1126/science.aba9757.
- 237 2. Leung K et al. *Lancet* 2020; DOI: [https://doi.org/10.1016/S0140-6736\(20\)30746-7](https://doi.org/10.1016/S0140-6736(20)30746-7).
- 238 3. Zhang J.J. et al. *Lancet Infect. Dis.* 2020; DOI: [https://doi.org/10.1016/S1473-](https://doi.org/10.1016/S1473-3099(20)30230-9)
239 [3099\(20\)30230-9](https://doi.org/10.1016/S1473-3099(20)30230-9).
- 240 4. Flaxman, S. et al. Estimating the number of infections and the impact of non-
241 pharmaceutical interventions on COVID-19 in 11 European Countries. DOI:
242 <https://doi.org/10.25561/77731>.
- 243 5. Tain H.Y. et al. *Science* 2020 ; 10.1126/Science.abb6105
- 244 6. Qiu J. *Nature* 2020; DOI: 10.1038/d41586-020-00822-x
- 245 7. Tang S.Y. et al. *Sci. Sin. Math.*. 2020; 50: 1-16, doi: 10.1360/SSM-2020-0053.
- 246 8. Tang B. et al. *Int. J. Inf. Dis.* 2020; DOI:
247 <https://doi.org/10.1016/j.ijid.2020.03.018>.
- 248 9. NHCC: National Health Commission of the People's Republic of China.
249 [http://www.nhc.gov.cn/xcs/yqtb/202003/097e6e91ecb6464ea69fd1a324c9b1b4.](http://www.nhc.gov.cn/xcs/yqtb/202003/097e6e91ecb6464ea69fd1a324c9b1b4.shtml)
250 [shtml](http://www.nhc.gov.cn/xcs/yqtb/202003/097e6e91ecb6464ea69fd1a324c9b1b4.shtml).
- 251 10. KCDC: Korea Centers for Disease Control and Prevention.
252 <https://www.cdc.go.kr/board/board.es?mid=a30402000000&bid=0030>.
- 253 11. MHLW: Ministry of Health, Labour and Welfare. Available from:
254 https://www.mhlw.go.jp/stf/newpage_09450.html.
- 255 12. CKDH: COVID-19 Knowledge & Data Hub. Available from:
256 <http://www.geodoi.ac.cn/COVID-19/index.aspx>.
- 257 13. Wikipedia. https://en.wikipedia.org/wiki/2020_coronavirus_pandemic_in_Iran.
- 258 14. Wikipedia.
259 https://en.wikipedia.org/wiki/2020_coronavirus_pandemic_in_Spain

260

261



262

263

264

265

266

267

268

269

270

271

272

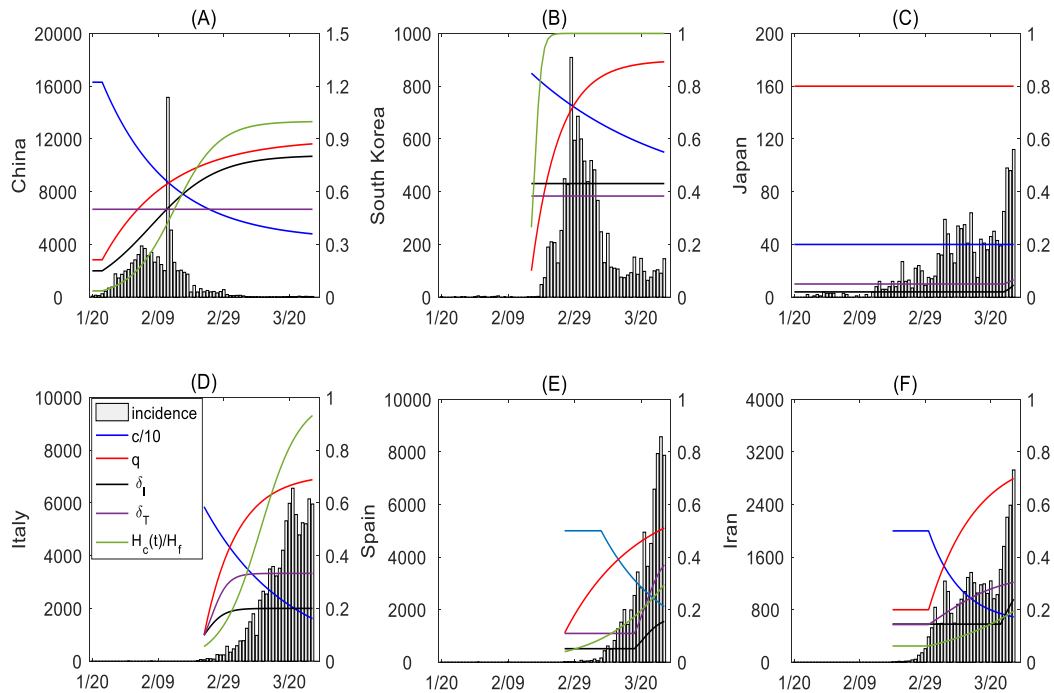
273

274

275

276

Fig.1: Data, curve fitting and effective reproduction numbers. (A). Numbers of newly reported cases for China, South Korea, Japan, Iran, Italy and Spain from 23 Jan to 27 March 2020. (B – G). Numbers of newly reported cases (red open circles) for China (B), South Korea (C), Japan (D), Italy (E), Spain (F) and Iran (G) and data fitting and 95% confidence intervals (gray) with predictions for one more month. Blue lines are the effective reproduction numbers (R_t) and their 95% confidence intervals.



277

278 **Fig.2: The synergistic effects of comprehensive intervention strategies and**
 279 **capacities of medical resources.** Numbers of newly reported cases for China (A),
 280 South Korea (B), Japan (C), Italy (D), Spain (E) and Iran (F) from 23 Jan to 27 March
 281 2020, and improving containment and mitigation measures including functions for
 282 contact rate (blue lines), quarantine rate (red), detection rate δ_I (black), detection rate
 283 δ_T (purple) and medical resources H_c (number of beds for each country, green). The
 284 contact rates have been divided by 10, and the numbers of beds have been divided by
 285 the carrying capacity H_f in each subplot.

286

287

288

289

290

291

292

293

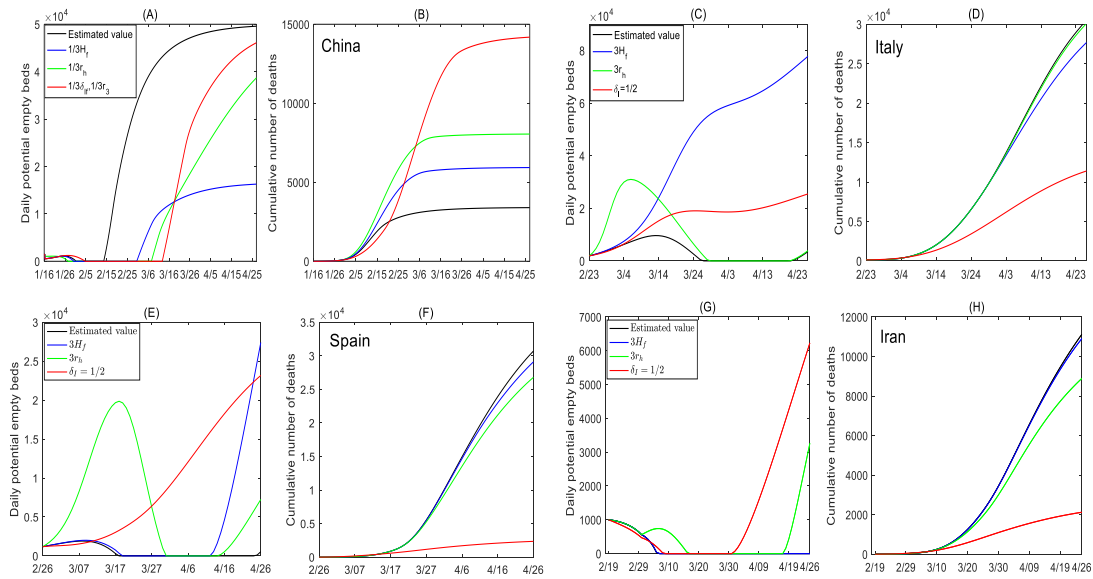
294

295

296

297

298



299

300

301

302

303

304

305

306

307

308

309

310

311

312

313

314

315

316

317

318

319

320

321

322

323

324

325

Fig.3: Sensitivity analyses reveal the relation between daily numbers of potential empty beds and cumulative numbers of deaths. The effects of the production capacity and reserve capacities of medical resources, and detection rates on runs on medical resources and cumulative numbers of deaths for China (A & B), Italy (C & D), Spain (E & F) and Iran (G & H). The daily potential numbers of empty beds were calculated from the formula $\max\{H_c(t) - H_2(t) - \theta H_1(t), 0\}$. The black curves in each subplot are generated by the baseline parameter values listed in Table S2. The values (Table 1) of daily potential numbers of empty beds and cumulative numbers of deaths on 26 April have been calculated to reveal when and how long the runs on medical resources could last, depending on the production capacities of medical resources and detection rates for each country, when each parameter value is reduced by 1/3.

326 **Table 1:** The effects of the production capacities and reserves of medical resources,
 327 and detection rates on runs on medical resources and cumulative numbers of deaths on
 328 26 April 2020.

Value of parameter	Daily potential empty beds (DPEB)			The cumulative number of death cases (CNDC)			Value of parameter	DPEB	CNDC
	Italy	Spain	Iran	Italy	Spain	Iran			
<i>Estimated value</i>	3539	545	0	30509	30709	11118	<i>Estimated value</i>	49598	3397
$3H_f$	77829	27400	0	27684 (-9.3%)	29099 (-5.2%)	10903 (-1.9%)	$1/3H_f$	16284 (-67.17%)	5933 (74.6%)
$3r_h$	3896	7254	3264	30103 (-1.3%)	26793 (-12.8%)	8890 (-20%)	$1/3r_h$	38705 (-21.96%)	8053 (137%)
$\delta_I = 1/2$	25487	23170	6322	11399 (-62.6%)	2350 (-92.3%)	2122 (-80.9%)	$1/3\delta_{If}$	46109 (-7.0%)	14187 (317.6%)
							$1/3r_3$		

329

330 **Table 2:** The effects of decreasing r_1 , r_2 , r_3 and r_h on the cumulative numbers of
 331 confirmed cases and cumulative numbers of deaths on 27 March 2020 in China and
 332 South Korea.

Cases	The cumulative number of confirmed cases		The cumulative number of deaths	
	China	South Korea	China	South Korea
Case C_1	8.256×10^4	9477	3329	170
Case C_2	1.0426×10^5 (+26.3%)	10693 (+12.8%)	5175 (+55.4%)	190 (+11.8%)
Case C_3	1.3881×10^5 (+68.1%)	12401 (+30.9%)	8618 (+158.8%)	217 (27.6%)
Case C_4	1.9892×10^5 (+141.0%)	14941 (+57.7%)	15396 (+362.4%)	251 (+47.6%)
Case C_5	3.1711×10^5 (+284.1%)	18962 (+100.0%)	30027 (+801.9%)	297 (+74.7%)
Case C_6	5.9333×10^5 (+618.7%)	25864 (+172.9%)	63657 (+1811.9%)	370 (+117.6%)

333 Note that r_1 , r_2 , r_3 , and r_h are the estimated values for corresponding countries, and for
 334 South Korea $r_3 = 0$ due to its constant diagnosis rate in Case C_1 . For Cases C_2 , C_3 , C_4 ,
 335 C_5 and C_6 , the four rates r_1 , r_2 , r_3 , and r_h were simultaneously reduced by 10%, 20%,
 336 30%, 40% and 50% respectively.

337

338

339

340

341

342

343

344

345 **Supplementary Materials:**

346 SM1. Model formulation

347 SM2. The definition of rate functions

348 SM3. Comparison of the intensity of control measures based on parameter values

349 SM4. The data and uncertainty analysis

350 SM5. Table for parameter definitions

351 SM6. Tables for parameter estimations

352 **Acknowledgements:**

353 This work was partially supported by the National Natural Science Foundation of

354 China (NSFCs: 11631012, 61772017), and by the Fundamental Research Funds for

355 the Central Universities (GK202007001, GK202003005, xzy032020028).

356

357

358

359

360 **Supplementary material (SM):** Effects of medical resource
 361 capacities and intensities of public mitigation measures on
 362 outcomes of COVID-19 outbreaks

363

364 This supplementary material (SM) provides detailed model description, definition
 365 of all rate functions, and comparisons of the intensities of control measures based on
 366 identified parameter values. In addition, medical resource limitations for each country
 367 are described and discussed in terms of numbers of hospital beds.

368

369 **SM1: The transmission model incorporating interventions**

370 In order to reveal the marked differences between the applications of various
 371 control strategies independently or simultaneously under medical resource limitation,
 372 we propose a generalized COVID-19 epidemic transmission dynamics model as
 373 shown in Fig.S1 (1,2):

$$\begin{cases}
 S' = -(c(t)\beta + q(t)c(t)(1 - \beta))SI/N - S(\beta_A c(t)A + \beta_H H_1)/N - \vartheta S + \lambda S_q, \\
 E' = (1 - q(t))c(t)\beta SI/N + S(\beta_A c(t)A + \beta_H H_1)/N - \sigma E, \\
 I' = \sigma \rho E - \alpha I - \delta_1(t)I, \\
 A' = \sigma(1 - \rho)E - \gamma_A A, \\
 S'_q = q(t)c(t)(1 - \beta)SI/N + (1 - \omega)\delta_T(t)T - \lambda S_q, \\
 T' = q(t)c(t)\beta SI/N + \vartheta S - \delta_T(t)T, \\
 H'_1 = \delta_1(t)I + \omega\delta_T(t)T - \min\{\theta H_1, \max\{(H_c(t) - H_2), 0\}\} - \gamma_1 H_1 - \alpha_1 H_1, \\
 H'_2 = \min\{\theta H_1, \max\{(H_c(t) - H_2), 0\}\} - \gamma_2 H_2 - \alpha_2 H_2, \\
 R' = \gamma_A A + \gamma_1 H_1 + \gamma_2 H_2.
 \end{cases} \quad (1)$$

375 In this model, $S, S_q, E, T, I, A, H_1, H_2, R$ represent the populations of susceptible (S),
 376 quarantined susceptible with contact tracing (S_q), exposed (E), quarantined suspected
 377 with contact tracing (T) including patients visiting fever clinics, infected (I) with
 378 symptoms, infected (A) but asymptomatic, people after a first medical visit but
 379 without a confirmed COVID-19 diagnosis and who are requested to quarantine at
 380 home (H_1), hospitalized and confirmed (H_2) and recovered (R). N denotes the total
 381 population, and $H_c(t)$ represents the capacity of hospital beds at time t which is used
 382 to describe the medical resource capacity. The detailed definitions can be found in
 383 section SM2.

384 In model (1), through contact tracing a proportion, q , of individuals exposed to the
385 virus is quarantined, and can either move to compartment T or S_q , depending on
386 whether they are infected or not. The other proportion, $1 - q$, consists of individuals
387 exposed to the virus who are missed from contact tracing and move to the exposed
388 compartment E when they become infectious, or else they stay in compartment S .
389 Further, we denote the transmission probability by β and the contact rate by c . Then,
390 the quarantined individuals, if infected (or uninfected), move to compartment T (or
391 S_q) at a rate of $\beta c q$ (or $(1 - \beta) c q$). Those who are not quarantined, if infected, will
392 move to compartment E at a rate of $\beta c (1 - q)$. We denote by constant ϑ the transition
393 rate from the susceptible class to the suspected compartment via general clinical
394 medication due to fever or other symptoms. Meanwhile, the transmissibility of
395 asymptomatic patients is lower than that of symptomatic patients, thus $\beta_A < \beta$.
396 Further, those confirmed but not hospitalized can transmit virus to their family
397 members, or others during their visits to health care facilities, and grocery stores etc.
398 so $\beta_H < \beta$.

399 We note that the data on suspected individuals and also most of the confirmed cases
400 come from the compartment T in China and South Korea. The suspected individuals
401 leave this compartment at a rate $\delta_T(t)$, with a proportion, ω , confirmed to be infected
402 by COVID-19 going to the compartment H_1 , whilst the other proportion, $1 - \omega$, proven
403 to be uninfected moves to the quarantined susceptible class S_q once recovered. People
404 confirmed with COVID-19 may not be hospitalized due to a limitation of hospital
405 beds, thus the term $\min \{ \theta H_1, \max \{ (H_c(t) - H_2), 0 \} \}$ is used to describe the
406 maximum number of newly hospitalized per day to maximize the hospital utilization,
407 which is a piecewise function according to the relationship between θH_1 and
408 $\max \{ (H_c(t) - H_2), 0 \}$, where θH_1 is the number of confirmed cases who are waiting
409 for beds on day t , $H_c(t)$ is the number of hospital beds at time t . Therefore,
410 $\max \{ (H_c(t) - H_2), 0 \}$ is the maximum number of remaining beds on the day. The
411 detailed definitions of all parameters are given in Table S1.

412 **SM2: Definition of rate functions**

413 As governments in various countries have been gradually strengthening their
414 protection measures and medical resources, and in particular, providing more and
415 more beds in response to the epidemic, we model the evolving number of beds by the
416 logistic growth model

$$417 \quad \frac{dH_c(t)}{dt} = r_h H_c(t) \left[1 - \frac{H_c(t)}{H_f} \right],$$

418 where r_h indicates the country-specific production capacity of medical resources in response to
419 emerging infectious diseases and H_f denotes the country-specific maximum number of beds that can
420 be provided during the disease outbreak. Therefore, these two parameters reflect the capacity of
421 medical resources of each country in response to COVID-19 outbreaks. In the early stage of an
422 outbreak, due to sufficient medical resources or insufficient understanding for the hospital bed
423 needs, the number of beds is basically constant. Therefore, solving the above logistic equation, we
424 have the number of beds on each day according to the following piecewise function:

$$425 \quad H_c(t) = \begin{cases} H_0, & t \leq T_c, \\ \frac{H_0 H_f}{H_0 + (H_f - H_0)e^{-r_h(t-T_c)}}, & t > T_c, \end{cases}$$

426 where H_0 indicates the number of initial beds that can be provided to patients with COVID-19 at the
427 beginning of the outbreak, and T_c denotes the critical time when each country starts to increase
428 medical resources including hospital beds. Such critical times were 23 January and 1 March 2020
429 for China and Iran, respectively, while T_c was zero for Italy, Spain and South Korea, i.e. at the
430 beginning of the epidemic the medical resources of these countries were constantly being
431 supplemented. In particular, before 25 March, due to the small number of confirmed cases, Japan
432 was not limited by any medical resources, so it is assumed that all confirmed cases were hospitalized
433 in time or isolated at home.

434 Since different containment and mitigation strategies have been implemented in different
435 countries with different critical times and intensities of strengthening prevention and control
436 measures (3-9), the functions related to contact, detection and quarantine rates in the model should
437 be defined as piecewise functions, and the corresponding parameter values can be used to reflect
438 the intensity at which control measures are implemented in each country. We define $c(t)$, $q(t)$,
439 $\delta_I(t)$ and $\delta_T(t)$ as follows. Note that the two functions $c(t)$ and $q(t)$ are fixed as constants for
440 Japan during the outbreaks, and the critical time for all rate functions defined in the following is 23
441 January for China, at the beginning of the epidemic for Italy.

442 In order to accurately describe the gradual strengthening of control strategies in this model, we
443 assume that with increasing intensity of a control strategy the contact rate $c(t)$ is a decreasing
444 function with respect to time t , given by (1,2)

$$445 \quad c(t) = \begin{cases} c_0, & t \leq T_c, \\ (c_0 - c_b)e^{-r_1(t-T_c)} + c_b, & t > T_c, \end{cases}$$

446 where c_0 denotes the baseline contact rate at the initial time with $c(0) = c_0$, c_b denotes the minimum
447 contact rate under the current control strategies with $\lim_{t \rightarrow \infty} c(t) = c_b$, where $c_b < c_0$, and r_1 denotes
448 how an exponential decrease in the contact rate is achieved. The critical time for Spain is 7 March
449 (5), and the critical times for other countries are the same as those in function $H_c(t)$.

450 Similarly, to characterize enhanced contact tracing we define $q(t)$ as an increasing function with
451 respect to time t , written as

$$452 \quad q(t) = \begin{cases} q_0, & t \leq T_c, \\ (q_0 - q_m)e^{-r_2(t-T_c)} + q_m, & t > T_c, \end{cases}$$

453 where q_0 is the initial quarantined rate of exposed individuals with $q(0) = q_0$ for China, South
454 Korea, Italy, Spain and Iran, q_m is the maximum quarantined rate under the current control strategies
455 with $\lim_{t \rightarrow \infty} q(t) = q_m$ and $q_m > q_0$, and r_2 represents how an exponential increase in the quarantined
456 rate is achieved. The critical times for each country are the same as those in function $H_c(t)$.

457 We also set the detection rate $\delta_I(t)$ as an increasing function with respect to time t , thus the
458 detection period $1/\delta_I(t)$ is a decreasing function of t with the following form:

$$459 \quad \frac{1}{\delta_I(t)} = \begin{cases} \frac{1}{\delta_{I0}}, & t \leq T_c, \\ \left(\frac{1}{\delta_{I0}} - \frac{1}{\delta_{If}}\right)e^{-r_3(t-T_c)} + \frac{1}{\delta_{If}}, & t > T_c, \end{cases}$$

460 where δ_{I0} is the initial rate of confirmation, δ_{If} is the fastest confirmation rate, and r_3
461 is the exponentially decreasing rate of the detection period. We define $\delta_I(0) = \delta_{I0}$

462 and $\lim_{t \rightarrow \infty} \delta_I(t) = \delta_{If}$ with $\delta_{If} > \delta_{I0}$. $\frac{1}{\delta_T(t)}$ can be similarly defined. Note that both

463 $\delta_I(t)$ and $\delta_T(t)$ are constants for South Korea, indicating that South Korea had a high
464 detection rate from the beginning of the epidemic. Due to the development of the
465 epidemic, Japan began to gradually improve its detection rate from 25 March, so the
466 critical time for both of these detection rate functions is 25 March. The critical time
467 for both detection rate functions $\delta_I(t)$ and $\delta_T(t)$ is 17 March in Spain (5). Similarly,
468 due to its limited medical resources, Iran first strengthened the detection rate of
469 suspected cases on 1 March (4), and then further expanded the detection range on 23
470 March, therefore the critical time for $\delta_T(t)$ is 1 March, and for $\delta_I(t)$ it is 23 March.
471

472 **SM3: Comparison of the intensity of control measures based on** 473 **parameter values**

474 **Detection rates** δ_I and $\delta_I(t)$, δ_T and $\delta_T(t)$

475 As the definition of the number of confirmed cases from the population waiting to
476 be tested (i.e. the T class) has not considered the process of passing the incubation
477 period, the baseline parameter values of $\delta_I(t)$ in some countries are greater than those
478 of $\delta_T(t)$, as shown in Table S2. The detection rates of Japan, Italy and Spain are
479 relatively lower than those for China and South Korea. However, Japan did not

480 gradually improve its detection rate until 25 March, while the detection rate for Iran
481 was increasing and finally tended to a level almost similar to that for China, which
482 indicates that Iran is constantly improving its detection rate.

483 **Quarantine intensity q or $q(t)$**

484 The isolation rate q in Japan has been very high since the outbreak, which fully
485 reflects the high intensity of self-isolation in Japan, with the strong self-discipline of
486 its citizens being one of the important factors resulting in the low level of the
487 outbreak. The final quarantine rates of China, South Korea and Iran tend to be close to
488 those of Japan with a relatively high growth rate r_2 . In contrast, the baseline values of
489 quarantine rates for Italy and Spain are relative low, and the growth rate for Spain is
490 smaller than those of all other countries.

491 **Contact rate c or $c(t)$**

492 There is no doubt that early in the outbreak in China, the number of contacts with
493 susceptible persons per infected person was the largest. The final contact numbers of
494 Italy, Spain and Iran are relatively low, which indicates that these countries have
495 escalated social distancing measures in the later period. If they continue to maintain
496 this level of measures for a long enough period, the outbreak can be halted. However,
497 Japan has always adopted a relatively mild prevention and control strategy, and its
498 exposure number has been maintained at a high level, while the limit value c_b of
499 South Korea is relatively large. This reveals that although the cumulative number of
500 reported cases in these two countries is not large at present, the number of newly
501 reported cases may increase repeatedly in the near future. This could be particularly
502 serious for Japan.

503 **Capacity of medical resources H_c and $H_c(t)$**

504 Due to the low cumulative number of confirmed cases and the low number of
505 newly reported cases, there is no problem of limited medical resources in Japan so far,
506 but with the development of the epidemic, whether there will be a run on medical
507 resources or not remains to be seen. The production capacity r_h of medical resources
508 in Italy is the largest except for South Korea, and then China. Compared with the
509 cumulative number of reported cases in China and Italy, as well as the capacity to
510 provide medical resources, i.e. the number of beds, it is clear that there is a run on
511 medical resources or a shortage of medical resources in Italy, which is much more
512 serious than that in China. Spain and Iran are the slowest in terms of capacity to
513 supplement medical resources, which may also be one of the reasons for the high

514 cumulative number of reported deaths in the two countries. It is also closely related to
515 the recovery rate discussed below.

516 **Recovery rate and disease-induced death rate of isolated cases at hospital** γ_2 and α_2

517 As for the recovery and mortality rates, since the epidemic data only report the
518 number of confirmed or in-hospital cases, we can only compare the recovery and
519 disease-induced death rates of isolated in-hospital patients here. The hospital
520 treatment time in South Korea, Spain, Italy and China is relatively short. The
521 mortality rate of patients in hospital is the highest in Spain, Iran and Italy, and the
522 lowest in China. The reason for the high mortality rate in Japan may be that only
523 severely ill patients are admitted to hospitals there.

524

525 **SM4: The data and uncertainty analyses**

526 We obtained the numbers of daily confirmed cases, cumulative numbers of deaths
527 and other data on COVID-19 in mainland China from NHCC (6); and those in South
528 Korea, Italy, Japan, Spain and Iran from the KCDC (7), MSPC (8) and WHO (9),
529 respectively. The critical times for strengthening or changing national prevention and
530 control measures can be found in publications (3-9).

531 In order to analyze the influence of the data randomness on parameter estimation
532 and model prediction, we assume that the epidemic data of each country follows a
533 Poisson distribution, and we randomly generate 1000 columns of datasets for fitting.
534 We then obtain the 95% confidence intervals for the curves generated by the real data
535 estimations in Fig.1 and Fig.S2.

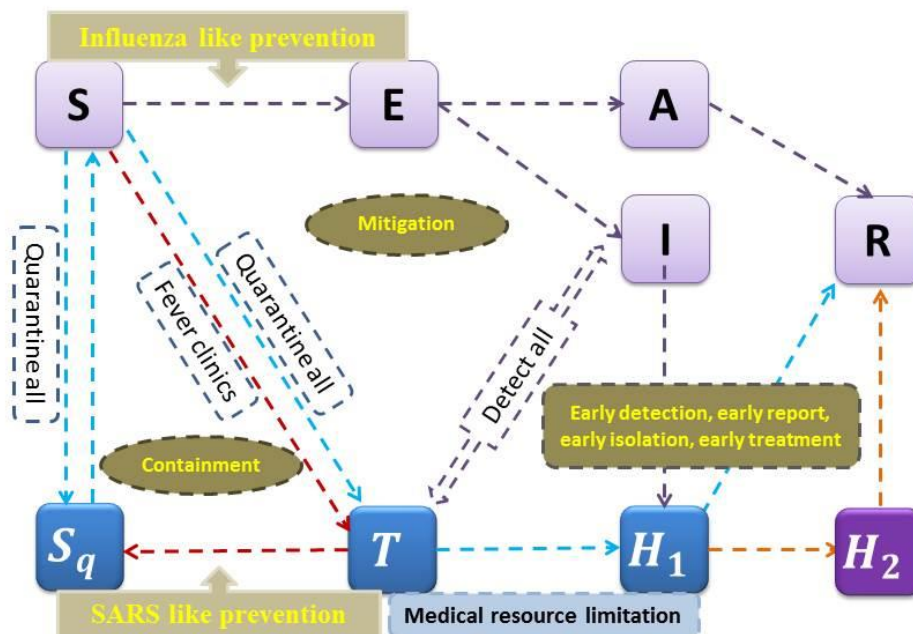
536

537 **References**

538

- 539 1. Tang B, Xia F, Tang S, et al. The effectiveness of quarantine and isolation determine the
540 trend of the COVID-19 epidemics in the final phase of the current outbreak in China. *Int.*
541 *J. Inf. Dis.* 2020, doi: <https://doi.org/10.1016/j.ijid.2020.03.018>.
- 542 2. Tang SY, Tang B, Bragazzi NL, et al. Analysis of COVID-19 epidemic traced data and
543 stochastic discrete transmission dynamic model (in Chinese). *Sci Sin Math.* 2020; 50: 1-
544 16, doi: 10.1360/SSM-2020-0053.
- 545 3. World Health Organization (WHO). Statement on the meeting of the International Health
546 Regulations (2005) Emergency Committee regarding the outbreak of novel coronavirus
547 (2019-nCoV). [https://www.who.int/news-room/detail/23-01-2020-statement-on-the-](https://www.who.int/news-room/detail/23-01-2020-statement-on-the-meeting-of-the-international-health-regulations-(2005)-emergency-committee-regarding-the-outbreak-of-novel-coronavirus-(2019-ncov))
548 [meeting-of-the-international-health-regulations-\(2005\)-emergency-committee-regarding-](https://www.who.int/news-room/detail/23-01-2020-statement-on-the-meeting-of-the-international-health-regulations-(2005)-emergency-committee-regarding-the-outbreak-of-novel-coronavirus-(2019-ncov))
549 [the-outbreak-of-novel-coronavirus-\(2019-ncov\)](https://www.who.int/news-room/detail/23-01-2020-statement-on-the-meeting-of-the-international-health-regulations-(2005)-emergency-committee-regarding-the-outbreak-of-novel-coronavirus-(2019-ncov)), 2020

- 550 4. Wikipedia. https://en.wikipedia.org/wiki/2020_coronavirus_pandemic_in_Iran.
551 5. Wikipedia. https://en.wikipedia.org/wiki/2020_coronavirus_pandemic_in_Spain.
552 6. NHCC: National Health Commission of the People's Republic of China.
553 <http://www.nhc.gov.cn/xcs/yqtb/202003/097e6e91ecb6464ea69fd1a324c9b1b4.shtml>.
554 7. KCDC: Korea Centers for Disease Control and Prevention.
555 <https://www.cdc.go.kr/board/board.es?mid=a30402000000&bid=0030>.
556 8. MSPC: Ministero della Salute, Protezione Civile.
557 <http://www.salute.gov.it/portale/nuovocoronavirus/homeNuovoCoronavirus.jsp>.
558 9. WHO: World Health Organization. Available from:
559 <https://www.who.int/emergencies/diseases/novel-coronavirus-2019/situation-reports>
560



561

562 Fig.S1: Flow diagram for the COVID-19 epidemic model incorporating
563 containment and mitigation measures, where the medical resources limitation is
564 described in terms of numbers of hospital beds.

565

566

567

568

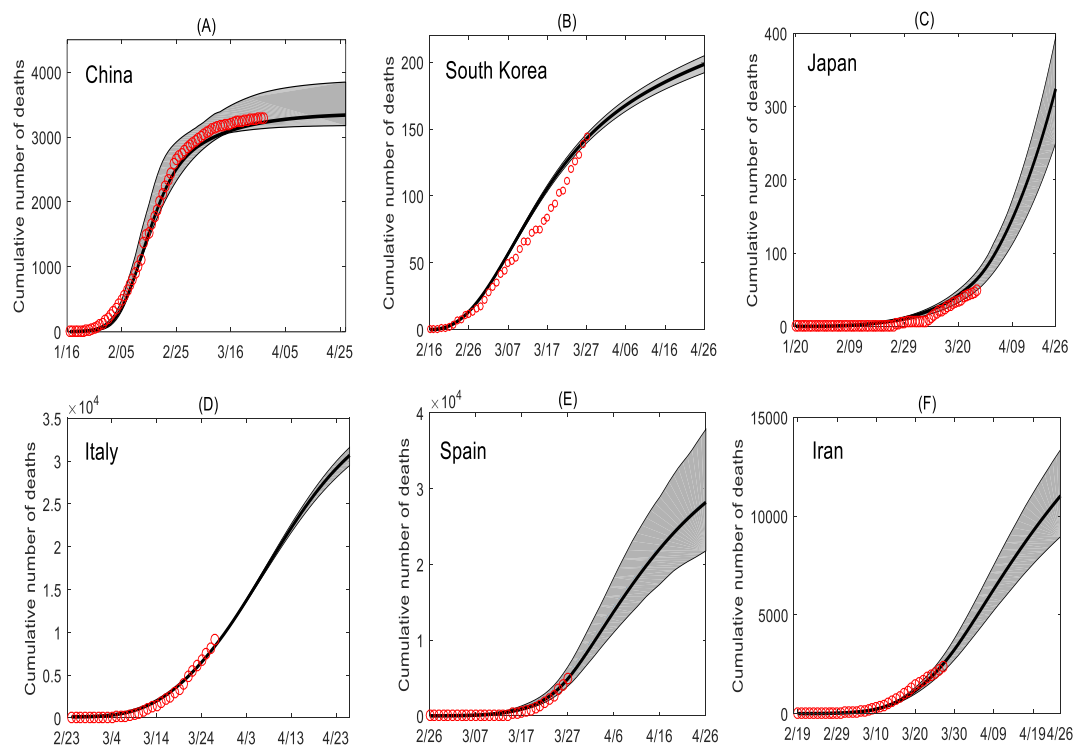
569

570

571

572

573



574

575 Fig.S2: Data fitting and 95% confidence intervals of cumulative numbers of deaths
576 for six countries indicated in each subplot.

577

578

579

580

581

582

583

584

585

586

587

588

589

590

591

592

593

594

595

596

597

598

599

600 **SM5. Table for parameter definitions**

601

602 **Table S1: Parameter definitions for the COVID-19 epidemics.**

Parameter	Definitions
$c(t)$	c_0 Contact rate at the initial time
	c_b Minimum contact rate under the current control strategies
	r_1 Exponential decreasing rate of contact rate
c	Constant contact rate
β	Probability of infected individuals transmission per contact
$q(t)$	q_0 Quarantined rate of exposed individuals at the initial time
	q_m Maximum quarantined rate of exposed individuals under the current control strategies
	r_2 Exponential increasing rate of quarantined rate of exposed individuals
q	Constant quarantined rate of exposed individuals
ϑ	Quarantined rate of susceptible individuals to the suspected class
β_A	Probability of asymptomatic individuals transmission per contact
β_H	Probability of quarantined infected individuals transmission per contact
ρ	Proportion of symptomatic infection
σ	Transition rate of exposed individuals to the infected class
λ	Rate at which the quarantined uninfected contacts were released into the wider community
$\delta_I(t)$	δ_{I0} Initial diagnosis rate of infected individuals
	δ_{If} Fastest diagnosis rate of infected individuals
	r_3 Exponential increasing rate of diagnosis rate of infected individuals
δ_I	Constant diagnosis rate of infected individuals
$\delta_T(t)$	δ_{T0} Initial diagnosis rate of quarantined individuals
	δ_{Tf} Fastest diagnosis rate of quarantined individuals
	r_4 Exponential increasing rate of diagnosis rate of quarantined individuals
δ_T	Constant diagnosis rate of quarantined individuals
ω	Confirmation ratio of quarantined exposed individuals
θ	Rate at which the confirmed infected individuals were hospitalized
γ_A	Recovery rate of asymptomatic infected individuals
γ_1	Recovery rate of confirmed infected individuals without hospitalization
γ_2	Recovery rate of hospitalized infected individuals
α	Disease-induced death rate of infected individuals
α_1	Disease-induced death rate of confirmed infected individuals without hospitalization
α_2	Disease-induced death rate of hospitalized infected individuals
$H_c(t)$	H_0 The number of available hospital beds at the initial time
	H_f Maximum capacity of hospital beds
	r_h Exponential increasing rate of hospital beds

Initial values	Definitions
$S(0)$	Initial susceptible population
$E(0)$	Initial exposed population
$I(0)$	Initial infected population
$A(0)$	Initial asymptomatic population
$T(0)$	Initial suspected population
$S_q(0)$	Initial quarantined susceptible population
$H_1(0)$	Initial confirmed infected population without hospitalization
$H_2(0)$	Initial hospitalized infected population
$R(0)$	Initial recovered population

603

604

605 SM6. Tables for parameter estimations

606

607 **Table S2:** Parameter estimates for the COVID-19 epidemics in China, South Korea,
608 Japan, Italy, Spain and Iran.

Parameter	Estimated values						Source	
	China	South Korea	Japan	Italy	Spain	Iran		
$c(t)$	c_0	12.2252	8.492	--	5.8547	5.0	4.995	Estimated
	c_b	3.2332	3.6005	--	0.0105	0.4649	1.4678	Estimated
	r_1	0.05	0.0237	--	0.0392	0.0532	0.101	Estimated
c	--	--	2.0	--	--	--	--	Estimated
β	0.1911	0.1911	0.1911	0.1911	0.1911	0.1911	0.1701(Est)	[1,2]
$q(t)$	q_0	0.2128	0.1003	--	0.1007	0.1112	0.1995	Estimated
	q_m	0.9	0.899	--	0.7106	0.6446	0.7963	Estimated
	r_2	0.05	0.1206	--	0.1	0.046	0.0697	Estimated
q	--	--	0.8	--	--	--	--	Estimated
ϑ	1.0×10^{-9}	0.0027	0.01	1.4561×10^{-9}	4.682×10^{-6}	4.98×10^{-9}	--	Estimated
β_A	0.001	0.0484	0.1028	0.15	0.1227	0.171	--	Estimated
β_H	0.001	0.0043	1.0051×10^{-4}	0.15	0.053	0.013	--	Estimated
ρ	0.45	0.95	0.4	0.4575	0.5556	0.6([7])	--	Estimated
σ	1/5	1/5	1/5	1/5	1/5	1/5	--	[8]
λ	1/14	1/14	1/14	1/14	1/14	1/14	--	[1]
$\delta_i(t)$	δ_{I0}	0.15	--	0.02*	0.099	0.0512	0.1447	Estimated
	δ_{If}	0.8071	--	0.4988	0.2001	0.1725	0.3337	Estimated
	r_3	0.1	--	0.2999	0.3495	0.3401	0.2998	Estimated
δ_I	--	0.4308	--	--	--	--	--	Estimated
$\delta_T(t)$	δ_{T0}	--	--	0.05*	0.0979	0.1093	0.1431	Estimated
	δ_{Tf}	--	--	0.4509	0.3329	0.4245	0.334	Estimated
	r_4	--	--	0.103	0.3995	0.3317	0.1	Estimated
δ_T	0.5	0.3835	--	--	--	--	--	Estimated

ω		0.1001	0.0089	0.2912	0.7999	0.7845	0.4931	Estimated
θ		0.4892	0.336	0.7732	0.3333	0.1677	0.3014	Estimated
γ_A		0.18	0.1807	0.1	0.1468	0.1442	0.2014	Estimated
γ_1		0.04	0.1359	0.0989	0.08	0.085	0.0498	Estimated
γ_2		0.08	0.0926	0.0667	0.0857	0.0903	0.0667	Estimated
α		0.01	0.005	1.0008 $\times 10^{-4}$	3.8099 $\times 10^{-4}$	0.0231	0.0212	Estimated
α_1		0.01	0.002	1.0066 $\times 10^{-4}$	0.0284	0.0201	0.012	Estimated
α_2		7.6724 $\times 10^{-4}$	0.0024	0.0053	0.01	0.0134	0.01	Estimated
$H_c(t)$	H_0	1500	796.679	--	1997.7	1200	999.1962	Estimated
	H_f	4.1968 $\times 10^4$	3.0065 \times 10^3	--	3.6 $\times 10^4$	3.0 $\times 10^4$	1.6235 $\times 10^4$	Estimated
	r_h	0.15	0.9728	--	0.1650	0.077	0.05	Estimated
Initial values	Estimated values						Source	
	China	South Korea	Japan	Italy	Spain	Iran		
$S(0)$	1.0×10^8	2.0651 $\times 10^6$	2.9985 $\times 10^6$	2.0×10^6	2.0×10^6	3.9945×10^6	Estimated	
$E(0)$	1000	999.919	10.0	2435.6	2500	149.2259	Estimated	
$I(0)$	400	99.6953	10.0	275.9334	400	209.0317	Estimated	
$A(0)$	414.5036	199.6778	79.9999	250.3936	280	140.2632	Estimated	
$T(0)$	2000	105.078	5.0	0.0001	0	0(Assumed)	Estimated	
$S_q(0)$	2000	7123(Data)	307.594	4.2×10^{-5}	7.4	0(Assumed)	Estimated	
$H_1(0)$	0	0	0	22	10	0	Data	
$H_2(0)$	28	21	0	80	10	0	Data	
$R(0)$	15	9	1	1	0	0	Data	

609 Note that, 'Est' means that the parameter values are estimated by fitting the models to the data when the source
 610 column indicates that they are not. '*' means the estimated values for δ_I and δ_T before 2020/3/25, otherwise δ_I and
 611 δ_T are increasing functions with respect to time t .

612
 613
 614